6th Annual International IEEE EMBS Conference on Neural Engineering
San Diego, California, 6 - 8 November, 2013

Dynamic Finite-Element Model of Axon Extracellular Stimulation

Fernando Henríquez, Dr. Carlos Jerez-Hanckes
Department of Electrical Engineering
School of Engineering
Pontificia Universidad Católica de Chile, Santiago, Chile

M.D. Fernando R. Altermatt
Department of Anesthesiology
School of Medicine
Pontificia Universidad Católica de Chile, Santiago, Chile

***Abstract*—We study the electrical influence of an electrode over an axon of nonzero thickness in time using a two-dimensional finite element formulation. Although our inspiration comes from the practice of peripheral nerve stimulation, other types of neural tissue excitation can benefit from the model. Our formulation combines a Hodgkin-Huxley model to account for nerve dynamics with electrostatic intra- and extracellular potentials. Thus, the influence of external electrode geometry and parameters can be addressed instead of simplifying them to point current sources. We show first numerical results for different extracellular stimuli and explore future enhancement directions.**

I. Introduction

Several applications in medicine and biology require the analysis of interactions between extracellular electrodes and electrically excitable tissue. Among these, Peripheral Nerve Stimulation (PNS) is of special importance in the practice of regional anesthesia [1], [2]. By means of a conducting needle connected to a current source, physicians try to evoke a motor response through particular nerves. Many works have tried to simulate the effects of the needle. Among them, Cantrell *et al.* [4] and Davis *et al.* [5] are able to compute the voltage and current field when a constant voltage is applied over the needle conductive surface but disregarding the actual electrode–nerve interaction. Rattay [6], [7], [8] studied the nerve's behavior by simplifying it to a one dimensional PDE called the *cable equation model* but considering the external electrode as a current point source. Ying *et al.* [9], using a finite element formulation, are able to study in detail the behavior of the transmembrane voltage when an external electric field is applied. However, since the external stimulation is incorporated through an external electric field, it is not able to take into account the electrode shape.

In this communication, we propose a mathematical model for the study of electrical interactions between an electrode and a neural structure: specifically, an axon. Our model is based on an finite element formulation coupled to a Hodgkin–Huxley model accounting for the non–linear nerve behavior [10], [11]. After discretization, a suitable numerical scheme is proposed to solve the problem. External stimulation is produced by a fixed amount of current flowing through the electrode's conducting surfaces.

II. Problem Model

We now present relevant assumptions and features to propose a well–posed mathematical formulation.

A. Cellular Membrane and Hodgkin–Huxley Equations

To model the axon's trans–membrane voltage we recall the Hodgkin–Huxley Model [10], [11]. Under this framework, the current per unit area flowing across the cellular membrane I and the transmembrane voltage V satisfy

$$\mathsf{I} = C_m \frac{\partial \mathsf{V}}{\partial t} + I_{\text{ion}}(\mathsf{V}, \mathbf{q}), \tag{1}$$

$$\frac{\partial \mathbf{q}}{\partial t} = \mathcal{M}(\mathsf{V}, \mathbf{q}). \tag{2}$$

The term I_{ion} represents the current flowing across the cellular membrane due the transport of ionic species across it; $\mathbf{q}$ denotes the vector of state variables representing the dynamic of the axon membrane; and, $\mathcal{M}(V, \mathbf{q})$ is the system of ordinary differential equations for $\mathbf{q}$ [12].

B. Problem Geometry

Our domain of interest is a subset of $\mathbb{R}^2$: the axon's membrane can be reduced to closed surface splitting the analysis region into intra- and extracellular domains, Ω_i and Ω_e, respectively, as show in Figure 1. The electrode's conducting surface is called Γ_t, being an equipotential surface through which a fixed amount of current flows. Surfaces Γ_u and Γ_d represent human skin, through which the current's tangential component can be non-zero. A grounded electrode is situated over Γ_r to close the current electric path, otherwise the problem has no physical meaning. To ensure this condition, the potential over Γ_r is set equal to zero.

C. Extracellular Stimulation

In this model, the extracellular current stimulation comes through the boundary Γ_t. If the external electrode is set to be a perfect conductor, the potential is constant and the total amount of current flowing across is a given value. Nevertheless, the current density at each point of Γ_t is unknown. Since we are dealing with a direct current electric conduction

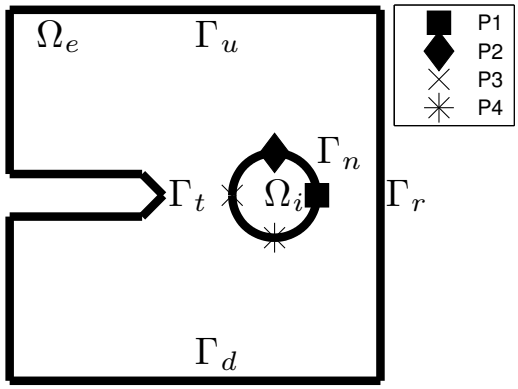

Fig. 1: Problem geometry. The domain of interest is separated into intra- and extracellular domains Ω_i and Ω_e, respectively. Boundary Γ_r is located at the right hand side whereas Γ_t represents the tip of the electrode. Surfaces Γ_u and Γ_n are sections of the outer boundary between Γ_t and Γ_r. Over the points P1, P2, P3 and P4 on Γ_n (the boundary representing the cellular membrane) the transmembrane voltage is measured as a function of time.

problem, the relation $\mathbf{J} = -\sigma\nabla u$ must hold. Integrating over an area A, one derives

$$\int_{\mathsf{A}} \mathbf{J}\cdot\hat{n}d\mathbf{s} = -\sigma\int_{\mathsf{A}}\frac{\partial u}{\partial\hat{n}}d\mathbf{s}. \tag{3}$$

Also, the total amount of injected current through A is

$$\mathsf{I_t} = -\int_{\mathsf{A}}\mathbf{J}\cdot\hat{n}d\mathbf{s} \tag{4}$$

Since this is a two dimensional approximation, all physical quantities portray do not change along the perpendicular direction to the plane. By choosing $\Delta\mathsf{L}$ as an arbitrary distance perpendicular to the plane of interest and redefining $\mathsf{A} := \Gamma_t \times \Delta\mathsf{L}$, we obtain

$$\mathsf{I_t} = -\int_{\mathsf{A}}\mathbf{J}\cdot\hat{n}d\mathbf{s} = \sigma\Delta\mathsf{L}\int_{\Gamma_t}\frac{\partial u}{\partial\hat{n}}d\mathbf{s}. \tag{5}$$

Thus, for a two dimensional formulation over Γ_t, it holds

$$\int_{\Gamma_t}\frac{\partial u}{\partial\hat{n}}d\mathbf{s} = \frac{\mathsf{I_{\Delta L}}}{\sigma} \tag{6}$$

where $\mathsf{I_{\Delta L}} = \mathsf{I_t}/\Delta\mathsf{L}$ is a current per length. Since Γ_t is a boundary of the extracellular domain, all the quantities must be interpreted as extracellular ones. The above discussion is only valid for a two-dimensional formulation. Whenever a three dimensional model is used, appropriate boundary condition can be deduced from the argumentation presented in this subsection.

D. Mathematical Formulation

Based on the quasi–static approximation of Maxwell's equations and representing the non–linear temporal behavior of the nerve through the Hodgkin–Huxley Model, it is possible to set up a consistent mathematical model. We aim to find $u_e \in H^1(\Omega_e)$ and $u_i \in H^1(\Omega_i)$, the corresponding Sobolev spaces [13], such that:

$$\begin{aligned}
\Delta u_i &= 0 \text{ in } \Omega_i, && (7)\\
\Delta u_e &= 0 \text{ in } \Omega_e, && (8)\\
\int_{\Gamma_t}\frac{\partial u_e}{\partial\hat{n}_e}d\mathbf{s} &= \frac{\mathsf{I_{\Delta L}}}{\sigma_e} && (9)\\
-\sigma_i\frac{\partial u_i}{\partial\hat{n}_i} &= \sigma_e\frac{\partial u_e}{\partial\hat{n}_e} = \mathsf{I} \text{ on } \Gamma_n, && (10)\\
u_i - u_e &= \mathsf{V} \text{ on } \Gamma_n, && (11)\\
\frac{\partial u_e}{\partial\hat{n}_e} &= 0 \text{ on } \Gamma_u\cup\Gamma_d, && (12)\\
u_e &= 0 \text{ on } \Gamma_r, && (13)
\end{aligned}$$

where

- u_i is the intra–cellular potential;
- u_e is the extra–cellular potential;
- V is the transmembrane potential across the cellular membrane Γ_n;
- I is the transmembrane current per unit area;

and, σ_i and σ_e are intra- and extracellular conductivities respectively. In addition to equations (7)–(13), we include a condition reflecting the fact of a constant potential over the electrode surface, i.e. u_e constant over the boundary Γ_t. This condition will be included directly in the finite element method's variational formulation by means of an adequate manipulation of the corresponding functional spaces.

III. Variational Formulation

Let us first define $H^1_1(\Omega_e)$ and $H^1_{\mathfrak{C}}(\Omega_e)$ the functional spaces satisfying:

$$\begin{aligned}
H^1_1(\Omega_e) &= \{u\in H^1(\Omega_e)|\ u|_{\Gamma_r} = 0 \text{ and } u|_{\Gamma_t} = 1\},\\
H^1_{\mathfrak{C}}(\Omega_e) &= \{u\in H^1(\Omega_e)|\ u|_{\Gamma_r} = 0 \text{ and } u|_{\Gamma_t} = \mathfrak{C}\in\mathbb{R}\}.
\end{aligned}$$

With these, condition (13) can already be included. Multiplying equation (7) by a test function $v_i \in H^1(\Omega_i)$ and recalling Green's first identity, we obtain

$$\int_{\Omega_i}\nabla u_i\cdot\nabla v_i d\mathbf{x} = \int_{\partial\Omega_i}\frac{\partial u_i}{\partial\hat{n}_i}v_i d\mathbf{s} = \int_{\Gamma_n}\frac{\partial u_i}{\partial\hat{n}_i}v_i d\mathbf{s}. \tag{14}$$

Repeating this procedure with equation (8), but using a test function $v_e \in H^1_1(\Omega_e)$ we have

$$\begin{aligned}
\int_{\Omega_e}\nabla u_e\cdot\nabla v_e d\mathbf{x} &= \int_{\partial\Omega_e}\frac{\partial u_e}{\partial\hat{n}_e}v_e d\mathbf{s} && (15)\\
&= \int_{\Gamma_t}\frac{\partial u_e}{\partial\hat{n}_e}v_e d\mathbf{s} + \int_{\Gamma_u\cup\Gamma_d}\frac{\partial u_e}{\partial\hat{n}_e}v_e d\mathbf{s}\\
&+ \int_{\Gamma_r}\frac{\partial u_e}{\partial\hat{n}_e}v_e d\mathbf{s} + \int_{\Gamma_n}\frac{\partial u_e}{\partial\hat{n}_e}v_e d\mathbf{s}. && (16)
\end{aligned}$$

Since v_e belongs to $H^1_1(\Omega_e)$, the integral over Γ_r in equation (16) must vanish. Also, due to the non-flux condition over $\Gamma_u\cup\Gamma_d$ (12), the related integral is equal to zero. The test function v_e is a constant equal to one over Γ_t, and consequently, by (9)

$$\int_{\Gamma_t}\frac{\partial u_e}{\partial\hat{n}_e}v_e d\mathbf{s} = \int_{\Gamma_t}\frac{\partial u_e}{\partial\hat{n}_e}d\mathbf{s} = \frac{\mathsf{I_{\Delta L}}}{\sigma_e}. \tag{17}$$

The variational representation of (8) including the current continuity over Γ_n, becomes

$$\int_{\Omega_e} \nabla u_e \cdot \nabla v_e d\mathbf{x} = \frac{\mathsf{I}_{\Delta\mathsf{L}}}{\sigma_e} - \frac{\sigma_i}{\sigma_e} \int_{\Gamma_n} \frac{\partial u_i}{\partial \hat{n}_i} v_e d\mathbf{s}. \tag{18}$$

Equation (11) must be included in a weak sense: multiplication by a test function $v_n \in H^{1/2}(\Gamma_n)$ yields

$$\int_{\Gamma_n} (u_i - u_e) v_n d\mathbf{s} = \int_{\Gamma_n} \mathsf{V} v_n d\mathbf{s}. \tag{19}$$

Finally, the original problem presented in Subsection II-D can be stated in the following way: find $u_i \in H^1(\Omega_i)$, $u_e \in H^1_{\mathfrak{C}}(\Omega_e)$ and $\frac{\partial u_i}{\partial \hat{n}_i} \in H^{1/2}(\Gamma_n)$ satisfying equations (14)–(18)–(19) for all $v_i \in H^1(\Omega_i)$, $v_e \in H^1_1(\Omega_e)$ and $v_n \in H^{1/2}(\Gamma_n)$. For the sake of simplicity, from we denote $u_n = \frac{\partial u_i}{\partial \hat{n}_i}$. The existence and uniqueness for both the continuous and discrete problems comes from the application of the Lax–Milgram lemma [13].

IV. Variational Formulation of the Hodgkin–Huxley Model

Let us assume V, $\mathbf{q}$, I_{ion} and $\mathcal{M}$ to be functions defined in $H^{1/2}(\Gamma_n)$. By multiplying equations (1)–(2) by a test function $v_n \in H^{1/2}(\Gamma_n)$ and integrating over Γ_n, we obtain a representation suitable to be coupled with the variational formulation developed in Section III. Aditionally, the time derivatives are approximated through an implicit Euler scheme and the underlying non–linear system is addressed by a fixed point procedure. Then, at time $t_j = j\Delta t$ ($j \in \mathbb{N}$) is imperative to solve iteratively

$$\begin{aligned} -\sigma_i \int_{\Gamma_n} (u_n)_j^k v_n d\mathbf{s} &= \frac{C_m}{\Delta t} \int_{\Gamma_n} (\mathsf{V}_j^k - \mathsf{V}_{j-1}) v_n d\mathbf{s} \\ &+ \int_{\Gamma_n} I_{\text{ion}}(\mathsf{V}_j^{k-1}, \mathbf{q}_j^{k-1}) v_n d\mathbf{s}, \end{aligned} \tag{20}$$

$$\begin{aligned} \frac{1}{\Delta t} \int_{\Gamma_n} \mathbf{q}_j^k v_n d\mathbf{s} &= \frac{1}{\Delta t} \int_{\Gamma_n} \mathbf{q}_{j-1} v_n d\mathbf{s} \\ &+ \int_{\Gamma_n} \mathcal{M}(\mathsf{V}_j^{k-1}, \mathbf{q}_j^{k-1}) v_n d\mathbf{s}, \end{aligned} \tag{21}$$

wherein

- V_j^k and $\mathbf{q}_j^k$: trans–membrane voltage at the time step j and fixed point iteration k.
- V_{j-1} and $\mathbf{q}_{j-1}$: trans–membrane voltage at the previous time step $j-1$.
- $(u_n)_j^k$: u_n at time step j and fixed point iteration k.

For each time t_j, the fixed point procedure must be repeated until the difference between consecutive steps lies below a given threshold.

V. Finite Element Discretization

Given admissible meshes $\mathcal{T}_i$ and $\mathcal{T}_e$ for Ω_i and Ω_e, respectively, we define piecewise linear basis functions φ_i such that $\varphi_i = 1$ at the i-th node and equals to zero on any other. Using the procedure proposed by Dular *et al.* [14], the nodes of $\mathcal{T}_e$ are split into two disjoint sets: those belonging to Γ_t and their complement, denoted $\mathcal{A}_t$ and $\mathcal{A}_{\overline{t}}$, respectively. We propose an adequate discrete *ansatz* for u_e:

$$u_e^h := \sum_{i \in \mathcal{A}_t} \alpha_i \varphi_i + \mathfrak{A} \underbrace{\sum_{i \in \mathcal{A}_{\overline{t}}} \varphi_i}_{=\varphi_{\mathcal{A}_{\overline{t}}}} \tag{22}$$

where $\alpha_i, \mathfrak{A} \in \mathbb{R}$ are the finite element approximation degrees of freedom for all nodes $i \in \mathcal{A}_t$. Then, u_e^h is an approximation coming from a discrete subspace of $H^1_{\mathfrak{C}}(\Omega_e)$. Moreover, $\{\varphi_i\}_{i \in \mathcal{A}_t}$ and $\varphi_{\mathcal{A}_{\overline{t}}}$ constitute a discrete subspace basis for $H^1_1(\Omega_e)$. Discrete approximations for u_i, u_n, V and $\mathbf{q}$ are given by the well-known expansion used in classical versions of the finite element method.

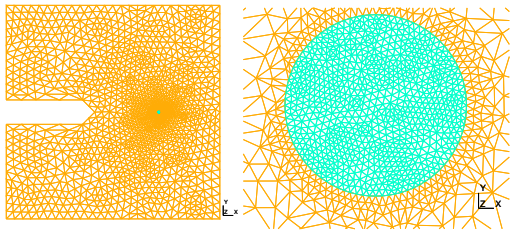

(a) Mesh $\mathcal{T}_e$ for Ω_e. The inner dot is the nerve's mesh.

(b) Mesh $\mathcal{T}_i$ for Ω_i.

Fig. 2: Admissible meshes $\mathcal{T}_i$ and $\mathcal{T}_e$ for Ω_i and Ω_e, respectively.

VI. Results and Discussion

Admissible meshes $\mathcal{T}_i$ and $\mathcal{T}_e$ are set up for Ω_i and Ω_e, as shown in Figure 2. Intra- and extracellular conductivities are $\sigma_i = 5$ mS/cm and $\sigma_i = 20$ mS/cm, respectively. Also, we set a time step $\Delta t = 0.01$ ms and simulate 10 ms of axon activity. Two situations are studied: (1) $\mathsf{I}_{\Delta\mathsf{L}} = 150$ mA/cm and (2) $\mathsf{I}_{\Delta\mathsf{L}} = -150$ mA/cm, for an axon diameter $d_A = 15$ μm. Figures 3 and 4 show the results for both situations.

Figures 3 and 4 portray classical shapes of the elicited transmembrane potential obtained through our formulation. Comparison of transmembrane voltages at different points on the axon's surface reveals same shapes but with significantly varying offsets. Even though differences in neural excitability are observed depending on the applied stimulation ($\mathsf{I}_{\Delta\mathsf{L}} > 0$ or $\mathsf{I}_{\Delta\mathsf{L}} < 0$), a comparison between Fig 3–(a) with 4–(c) and Fig 3–(c) with 4–(a) reveals a spatial inversion of the solution when changing the polarity of the excitation. Thus, this model is not able to predict differences in excitability as the ones observed in the experimental practice [15].

VII. Conclusions

A two-dimensional numerical framework to deal with interactions between a neural structure, as an axon, and an extracellular electrode have been developed in the present work. Among the objectives achieved, our finite element formulation is able to represent the external stimulation as a fixed amount of current flowing across the electrode's surface. Also, there is no need to reduce the external stimulation to a constant electric

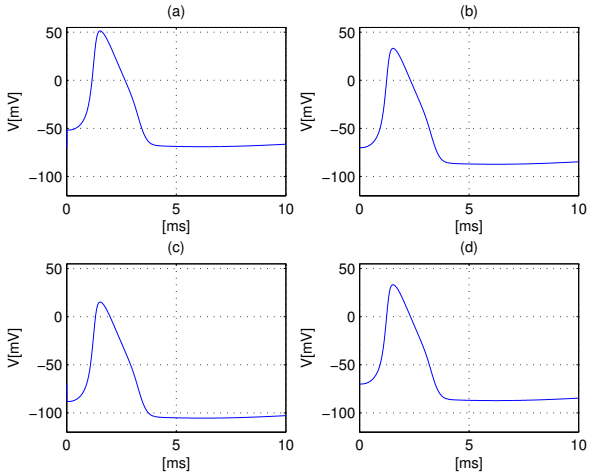

Fig. 3: Transmembrane voltage measured between $t_i = 0$ms and $t_f = 10$ms using $\mathsf{I}_{\Delta\mathsf{L}} = 150$mA/cm for differentes points over the cellular membrane or the surface Γ_n. Figures (a), (b), (c) and (d) are the trans-membrane voltage measured at points P1, P2, P3 y P4 as showed in Figure 1.

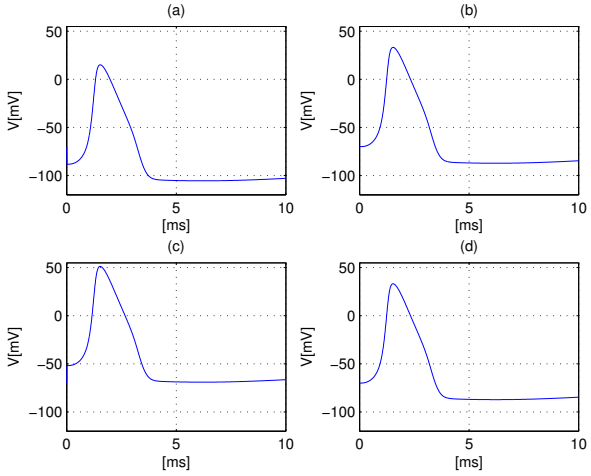

Fig. 4: Transmembrane voltage measured between $t_i = 0$ms and $t_f = 10$ms using $\mathsf{I}_{\Delta\mathsf{L}} = -150$mA/cm for differentes points over the cellular membrane or the surface Γ_n. Figures (a), (b), (c) and (d) are the trans-membrane voltage measured at points P1, P2, P3 y P4 as showed in Figure 1.

field, as proposed by Ying *et al.* [9] or a current point source as done by Rattay [6], [7], [8]. Future work will concern three-dimensional models excitation of multiple axons as well as a search of better models to address differences in excitability due to changes in polarity of the external stimulus.

ACKNOWLEDGEMENTS

The present work was funded by the VRI Interdisciplina fund No. 11/2011 by Pontificia Universidad Católica de Chile and FONDECYT Iniciación Grant No. 11121166.

REFERENCES

[1] C. Bollini, F. Cacheiro. "Peripheral Nerve Stimulation". *Techniques in Regional Anesthesia and Pain Management*, vol. 3, no. 10, pp. 7988, 2006.

[2] C. Pham-Dang, O. Kick, T. Collet, F. Gouin, M. Pinaud. "Continuous peripheral nerve blocks with stimulating catheters". *Regional Anesthesia and Pain Medicine*, vol. 28, no. 2, pp. 8388, 2003.

[3] N. Sepulveda, J. Wikswo, D. Echt. "Finite Element Analysis of Cardiac Defibrillation Current Distributions". *IEEE Transactions on Biomedical Engineering*, vol. 37, no. 4, 1997.

[4] M. Cantrell, W. Grill, S. Klein, "Computer-based finite element modeling of Insulated tuohy needles used in regional anesthesia", *Anesthesiology*, vol. 110, no. 6, pp. 1229–1234, 2009.

[5] J. Davis, N. Anderson, J. Ramirez, F. Kayser Enneking, M. Meisel. "Finite-difference modeling of the anisotropic electric fields generated by stimulating needles used for catheter placement", *IEEE Transactions on Biomedical Engineering*, vol. 54, no. 7, pp. 1186–1190, 2007.

[6] F. Rattay. "Analysis of Models for External Stimulation of Axons". *IEEE Transactions on Biomedical Engineering*, vol. 33, no. 10, pp. 974–977, 1986.

[7] F. Rattay. "Analysis of Models for Extracellular Fiber Stimulation". *IEEE Transactions on Biomedical Engineering*, vol. 36, no. 7, pp. 676–682, 1989.

[8] F. Rattay. *Electrical Nerve Stimulation. Theory, Experiments and Applications*. Vienna, Austria: Springer–Verlag, 1990, ch. 57, pp. 73139.

[9] W. Ying, C.S. Henriquez. "Hybrid Finite Element Method for Describing the Electrical Response of Biological Cells to Applied Fields". *IEEE Transactions on Biomedical Engineering*, vol 54, no. 4, April 2007.

[10] A.L. Hodgkin and A.F. Huxley. "A quantitative description of membrane current and its application to conduction and excitation in nerve". *The Journal of Physiology*, vol. 117, no. 4, pp- 500–544, 1952.

[11] A.L. Hodgkin, A.F. Huxley AF, B. Katz. "Measurement of current–voltage relations in the membrane of the giant axon of Loligo". *Journal of Physiology*. vol. 116, no. 4, pp. 424–448, 1952.

[12] S. Doi, J. Inoue., Z. Pan, K. Tsumoto. *Computational Electrophysiology*. Tokyo, Japan: Springer Series, A First Course in In Silico Medicine, vol. 2, 2010.

[13] O. Steinbach, *Numerical approximation methods for elliptic boundary value problems*, Springer–Verlag, New York, 2008.

[14] P. Dular, W. Legros. "Coupling of Local and Global Quantities in Various Finite Element Formulations its Application to Electrostatics, Magnetostatics and Magnetodynamics", *IEEE Transactions on Magnetics*, vol. 34, no. 5,1998.

[15] J. Li, X. Kong, S.N. Gozani, R. Shi, R. Borgens. "Current–Distance Relationships for Peripheral Nerve Stimulation Localization", *Anesthesia & Analgesia*, vol. 112, no. 1, 2011.